# Enhancement of an Aeroelastic Solver for Design Optimization of HAWT

## Final report

*University Roma Tre*

### *Introduction*

This report summarizes the activities performed by University Roma Tre (hereinafter UR3) Rotorcraft group during the period *September-2013/June-2014*, as agreed with *AIRWORKS-ENGINEERING* (hereinafter AW).

It stems from the results achieved in the previous two years, described in Refs.[1] and [2]. The final goal was the enhancement of the aeroelatic-design optimization tool developed in the previous years. The aim was to improve both the availability and the quality of the aerodynamic models, of the blade-box modeling, and of the optimization criteria, in order to be more useful and a more direct aid in the preliminary-design phase of HAWT blades layout. Further, the solver has been given a GUI, currently at its Beta-Version, to be usable from a common user in a friendly way.
UR3 and AW cooperated to assemble such a tool as follows in brief:

- **The aeroelastic module provided by UR3, namely Tiltaero (TA), was enhanced with more aerodynamic modeling capabilities**, apart from AW's Aerodyn (Adyn) module, providing the user a set of choices depending on the desired analysis. The former data files required from TA and Aerodyn were of course merged or substituted to be suitable for every chosen model.

- **AW developed both a structural model of the blade-box and a tool for the sectional structural strenght analysis**. In general the blade-box model provides the sectional properties necessary for the aeroelastic analyses starting from real design values, like internal thicknesses, spar width and cells number.

- **A new solver was assembled, named AEP (Annual Energy Production), able to use TA to compute a power curve and the following AEP for a HAWT** with assigned nominal power, RPM and a given wind speed statistic distribution, with a given regulation strategy (pitch or stall).

- **The design optimization tool (MDO) described in [2] was integrated and enhanced with the new and the enhanced modules**, thus changing the overall design process in terms of constraints, design variables and objective functions.

- **UR3 designed and developed a GUI** to access both to separate performance and structural analyses capilities of TA, and to use the design tool.

## Aerodynamic Modelling Enhancement

### Tiltaero General Presentation

For the sake of clearness a short description of TA from Ref. [2] is here recalled.

TA is one of the aeroelastic codes developed by UR3 Rotorcraft group. It was applied in the past for several kind of aeroelastic analyses on rotary wing aircraft, both helicopters and tiltrotors. For an accurate description Refs. [5]-[6] are recommended. Basically, concerning the rotor, it is based on a beam model for the structural definition of the blades undergoing moderate deflections, and can use increasing refinements for the aerodynamics description, which, however, can be described by 2D standard models (Ref. [4]). TA's main functionality is computing the aeroelastic response of rotorcraft undergoing straight flight, which can be generally identified by steady-periodic conditions. It can count on a very accurate kinematic modelling for every section of the blade, both related to rigid body motion, and on elastic in-plane and out-plane deflections, together with torsional rotations. The rotor can be kinematically and dynamically connected to its support, which can as well be a deformable pylon with its nacelle. The kinematics directly connects to external, inertial and aerodynamic, and internal elastic loads related to each section, which describe a set of integro-partial, differential equation for coupled biflexion-torsion deflections whose very general form is, infact:

$$\mathbf{f}_{elas} + \mathbf{f}_{iner} + \mathbf{f}_{aerod} = \mathbf{0} \tag{1}$$

TA includes a fully-variable structural-characteristics layout, three-axis hinges, structural couplings and curved elastic axis among others. The solution of the differential equations related to each degree of freedom described (elastic bending and torsional deflections, but also angular rotations due to hinges, as well as dofs related to hub and drive-train elasticity) is obtained by following a modal approach and the known *Galerkin method* for spatial integration. Different analyses can be executed:

- Time-Marching integration.

- Harmonic Balance Response, which is a technique for the time solution of an inherently periodic system (it is very usefull as it skips the transient solution, thus resulting very fast compared to time marching solutions). Given the nonlinear nature of the aeroelastic system, the solution is reached iteratively based on a standard Newton-Raphson numerical scheme.

- Eigenvalue Analysis

### Tiltaero Aerodynamic Models

Figure 1 shows a sketch of TA possible user choices in terms of aerodynamic modeling. Briefly, two main models are available:

1. Steady Aerodynamics

2. Unsteady Aerodynamics with optional Stall models

**The Steady Aerodynamics is provided by Adyn** coupled with TA structural dofs, as described in [1] and [2].

The aerodynamic forces are given by coefficient tables that the user must provide, optionally with the new feature of different values for different Mach numbers for each profile. The aerodynamic lift, drag and torsion moment are as follows:

$$\begin{cases} L(x,t) = \dfrac{1}{2}\rho V^2 c(x) c_l(x, Ma, \alpha(t)) \\[2mm] D(x,t) = \dfrac{1}{2}\rho V^2 c(x) c_d(x, Ma, \alpha(t)) \\[2mm] M(x,t) = \dfrac{1}{2}\rho V^2 c(x)^2 c_m(x, Ma, \alpha(t)) \end{cases} \qquad (2)$$

**The Unsteady Aerodynamic is derived by a standard Beddoes-Leishman (BL) formulation** for 2D aerodynamics [7], extended to 3D with a UR3's original formulation for spatial integration already tested and published in [8] and [9]. It implies the sum of two additional variables per section describing the unsteady shed vorticity generated by time-varying angles of attack.

If stall is activated further 10 dofs are introduced. They include the dynamic of delayed pressure, of the point of detachment along the profile's chord, of the impulsive and non-circulatory loads and of the vortex possibly developing from leading edge separation. The overall aerodynamic model can be summarized by the following first order differential system to be coupled to Eq. 1 through the terms relating the $\alpha$ angle, which in turn depends on structural dofs. Here **x** represent the aerodynamic added states, whilst the **q** are the strucural dofs. The coupled aeroelastic system is described in 3.

$$\begin{cases} \dot{\mathbf{x}} = \mathbf{A}\mathbf{x} + \mathbf{B}\alpha(\mathbf{q}, \dot{\mathbf{q}}) \\[2mm] \mathbf{f_{elas}}(\mathbf{q}) + \mathbf{f_{iner}}(\ddot{\mathbf{q}}, \dot{\mathbf{q}}, \mathbf{q}) + \mathbf{f_{aerod}}(\ddot{\mathbf{q}}, \alpha(\dot{\mathbf{q}}, \mathbf{q}), \mathbf{x}) = \mathbf{0} \end{cases} \qquad (3)$$

A significant effort has been made to enable the user to have an appropriate control on the system dimension and the following computing time. It is possible to choose whether the application is *static* (e.g. axial flow during performance calculation) or not, thus eliminating dofs related to impulsive and non-circulatory terms, which only make sense to appear in *dynamic*, unsteady conditions. Moreover, as impulsive terms equations are governed by time constants to be determined, if these data have not been acquired, the non-circulatory terms can be given by a subset of theodorsen definitions (Ref. [4]), related to section deformations and dofs. Finally, it is worth highlighting that the leading edge vortex generation is a phenomenon which can not always
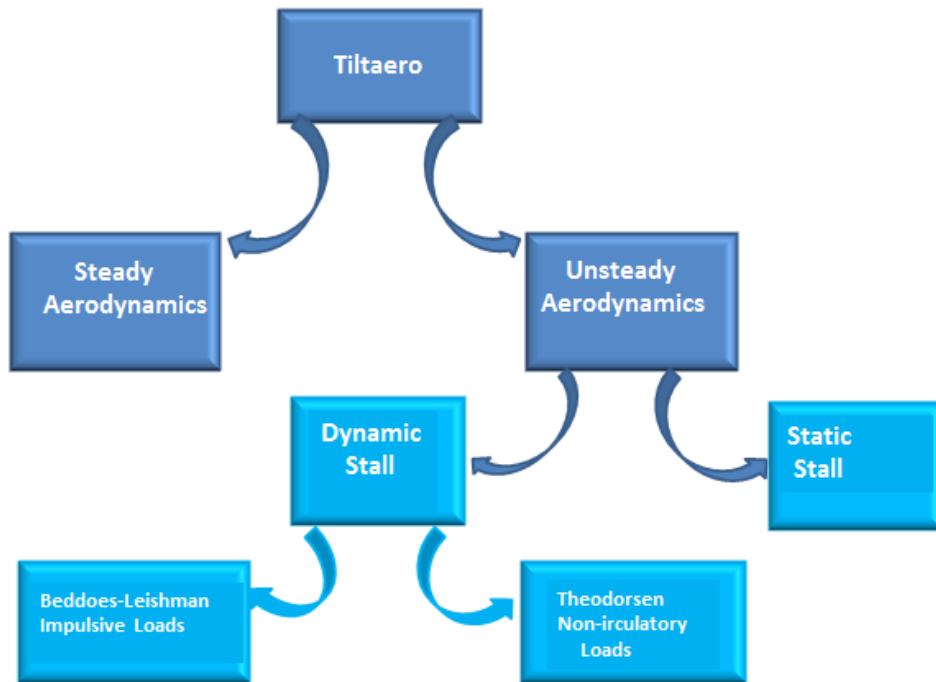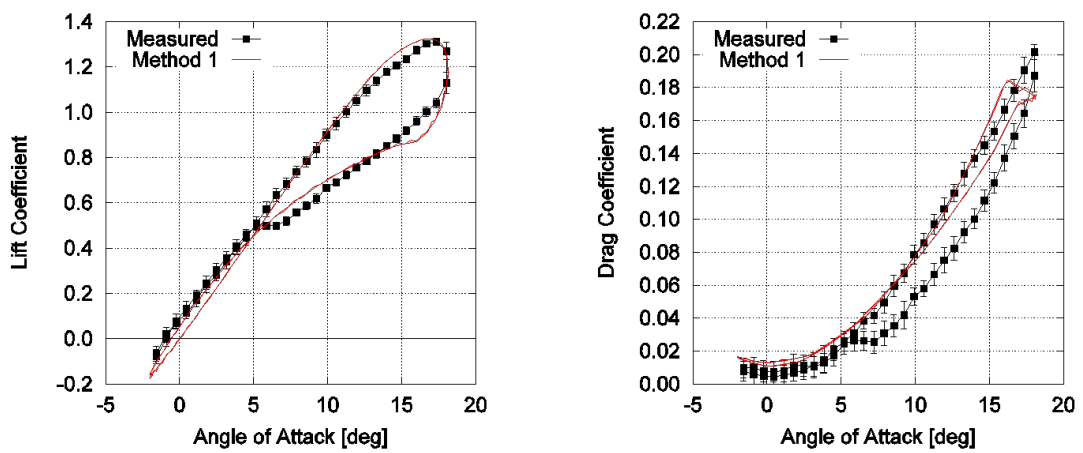
Figure 1: Tiltaero Aerodynamics Sketch



Figure 2: Example of Dynamic stall Cl-Cd identification

be described in the rotor revolution time used for Harmonic balance, so it is activated by default only in time-marching analyses. Method 1 in the figure above is an example of 2D coefficient obtained with the unsteady aerodynamics module, with a very good comparison with respect to experimental data.

**High angles of attack and the 3D corrections.**

1. No matter which model is used the aerodynamic coefficients are automatically determined based on overall 3D flat-plate theory over an imposed range of angles of attack, usually corresponding to the matching point with available coefficient-table data. Indeed, when the prescribed angle of attack $\alpha_{hi}$ is exceeded in module, the known flat plate relation are used, also corrected to take into account profile asymmetry when needed. The entire angle range is summarized in table 1

| $\alpha$ | $c_l$ | $c_d$ |
|---|---|---|
| $\alpha_{hi} < \alpha \leq \pi/2$ | $0.5\, c_D^{90} \sin 2\alpha$ | $c_D^{90} \sin^2(\alpha)$ |
| $\pi/2 < \alpha \leq \pi - \alpha_{hi}$ | $-0.5\, c_D^{90} \sin 2\alpha$ | $c_D^{90} \sin^2(\alpha)$ |
| $\pi - \alpha_{hi} \leq \alpha < \pi$ | $C_1 c_l(\alpha_{hi})(\alpha - \pi)/\alpha_{hi}$ | $c_D^{90} \sin^2(\pi - \alpha)$ |
| $-\pi/2 < \alpha \leq -\alpha_{hi}$ | $-C_1 0.5 c_D^{90} \sin(-2\alpha)$ | $c_D^{90} \sin^2(-\alpha)$ |
| $-\pi + \alpha_{hi} < \alpha \leq -\pi/2$ | $C_1 0.5 c_D^{90} \sin(\alpha + \pi)$ | $c_D^{90} \sin^2(\pi + \alpha)$ |
| $-\pi < \alpha \leq -\pi + \alpha_{hi}$ | $C_1 c_l(\alpha_{hi})(\pi + \alpha)/\alpha_{hi}$ | $c_D^{90} \sin^2(\pi + \alpha)$ |

Table 1: $C_l / C_d$ Vs $\alpha$

Here $C_1$ accounts for coefficient reduction due to profile asymmetry, by convention it is defined equal to 0.7.
$c_D^{90}$ is the drag coefficient of a flat plate at 90 degrees. In a 2D case it is $c_D^{90} = 2$, but in 3D application experimental relations have been found, depending on the aspect ratio $AR$ of the blade. The user can choose by data file among three different laws, these are in the order:

$$\begin{cases} c_D^{90} = 1.11 + 0.018 AR \\ c_D^{90} = 1.45 + 0.61(1 - e^{-2/AR}) \\ c_D^{90} = 1.45 + 0.61 \tanh(12.22/AR) \end{cases} \tag{4}$$

Anyway an automatic correction prevents to be $c_D^{90} > 2$.

2. Corrections are applied to the coefficients to account for centrifugal effects based on Snell model. Particularly, the reduction of rotating sectional lift coefficient near the tip, due to the decrease of radial suction and gradient of dynamic pressure appeared to have a noticeable effect. Its expression was suggested in [10]:

$$Cl_{rot-tip} = Cl_{non-rot} - (\lambda_{eff}/(1 + \lambda_{eff}^2 0))^2 e^{-1.5 AR_{out}} (Cl_{pot} - Cl_{non-rot}) * Cl_{non-rot}/Cl_{pot} \tag{5}$$

where $Cl_{non-rot}$ is the table data, $\lambda_{eff}$ is the tip speed ratio, $AR_{out}$ is the local aspect ratio (i.e. computed from the considered section to the tip) and $Cl_{pot}$ is the known potential lift coefficient. Fig. 3 shows performance
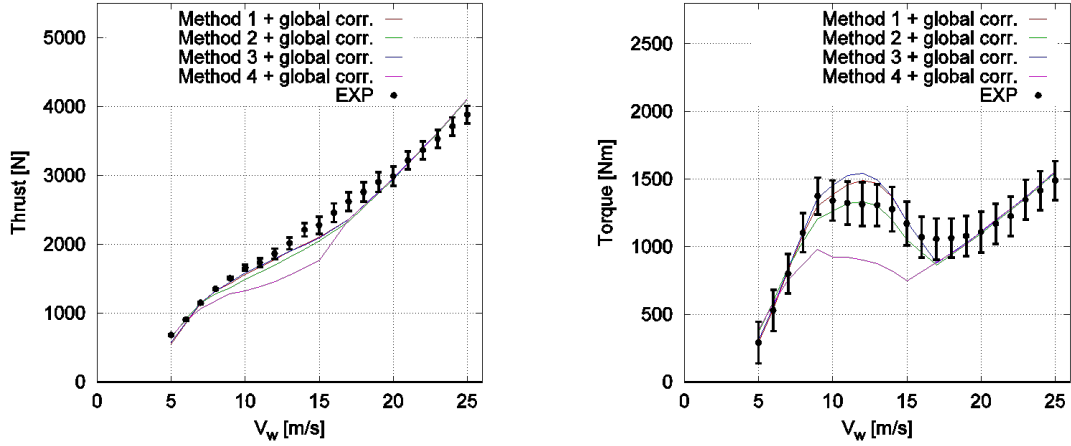


Figure 3: Example of Performance computation up to complete stall condition

computation from fully attached flow to deep stall conditions.

3. Two new user-optional trailed vorticity induced velocity models have been provided, apart from the one previously included in Adyn.

   - Induced Velocity given from standard BEMT theory for HAWT
   - Induced Velocity from users' own database

The BEMT induced velocity is a standard literature model for the inflow. The union of Momentum and Blade Element theories yields to a model describing two components of induced velocity, normal and parallel to the plane of rotation (see Fig.4). This components are computed by an iterative process and are described by two *induction factors* $a$ and $a'$, such as

$$\begin{cases} V_{inflow}^n = -aV_0 \\ V_{inflow}^p = a'\Omega x \end{cases} \tag{6}$$

As a reference we can cite [11] where the process is fully described. The process also takes into account Prandtl's hub and tip loss factors. For the sake of completeness, here are reported the resulting relations, obtained respectively from axial and angular momentum :

$$\begin{cases} a = \sigma C_n/(4F\sin^2(\phi) + \sigma C_n) \\ a' = \sigma C_t/(4F\sin(\phi)\cos(\phi) - \sigma C_t) \\ F = F_{hub}F_{tip} \; ; \; \sigma = (N_{blade}c(x))/(2\pi x) \end{cases} \tag{7}$$

It is worth to remind that the first equation of 7 has a limit for $a = 0.5$, when the equation yields to an impossible solution of reverse flow in the
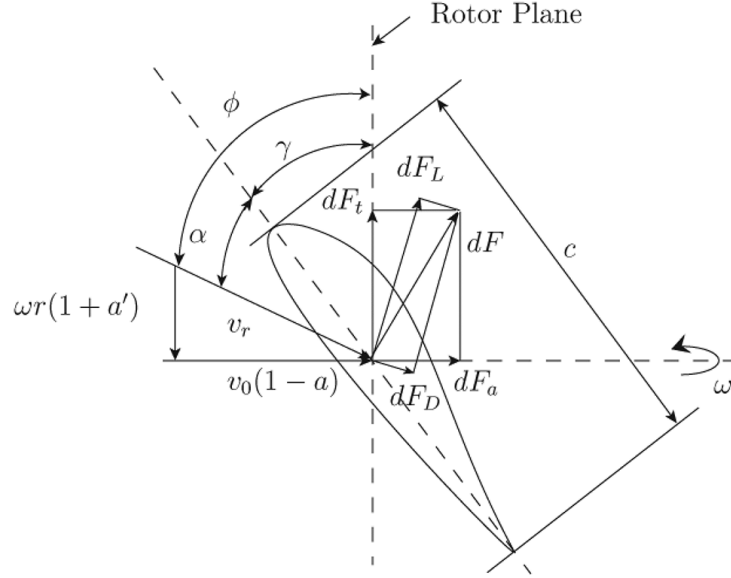
6

Figure 4: Section velocities and inflow

stream tube. This is bypassed by using an empirical relation for conservative values of $a > 0.4$, the chosen relation comes from the solution of the following system:

$$\begin{cases} dC_T = \sigma(1-a)^2 C_n/(F\sin^2(\phi)) \\ dC_T = \dfrac{8}{9} + \left(4F - \dfrac{40}{9}\right)a + \left(\dfrac{50}{9} - 4F\right)a^2 \end{cases} \tag{8}$$

In the previous formulas $C_n$ and $C_t$ are normal and tangential sectional force coefficients, as $dC_T$ is an 'annular' $C_T$ value

**Windshear Modeling**

Finally a windshear model has been introduced. At the moment a deterministic wind profile is implemented, as described by standard international regulation IEC-61400-1. Both NPT, normal profile type, and EPT, extreme profile type, were implemented, defined in the order as

$$V_w(z) = V_{hub}(z/z_{hub})^{0.2}; V_{hub} = V(z_{hub}) \tag{9}$$

and

$$\begin{aligned} V_{50y} &= 1.4V_{ref}(z/z_{hub})^{0.11} \\ V_{1y} &= 0.8V_{50y} \end{aligned} \tag{10}$$

EPT can use extreme wind experienced in a 50 years ($V_{50y}$) or 1 year ($V_{1y}$) period. The reference wind speed $V_{ref}$ depends on the class of the turbine, as shown in the table below.

| Wind turbine class | | I | II | III | S |
|---|---|---|---|---|---|
| $V_{ref}$ | (m/s) | 50 | 42,5 | 37.5 | Values |
| A | $I_{ref}$ (-) | | 0,16 | | specified |
| B | $I_{ref}$ (-) | | 0,14 | | by the |
| C | $I_{ref}$ (-) | | 0,12 | | designer |

Figure 5: $V_{ref}$ according to HAWT classes

### *AEP Module*

Forecasting the annual energy production is crucial when dimensioning and designing a site for wind power extraction. Indeed, it is one of the most used figure of merit and objective function of optimization attempts for wind turbines.

AEP is a module designed to compute annual energy production. It can be used :

- in an optimized design process, using aep as objective function

- in a performance analysis, also defining the pitch angle required to keep nominal power once it is reached.

To compute the aep both the blade configuration and the velocity of the wind must be known. Wind speed during the year is elaborated in terms of probability density function, usually provided by a Releigh or Weibull distribution (depending on the coefficients).

$$f(u) = \frac{k_w}{A_w} u^{k_w - 1} e^{(-u/A_w) k_w} \tag{11}$$

aep is the area below the power curve P(u) in Fig. 7, multiplied by the working
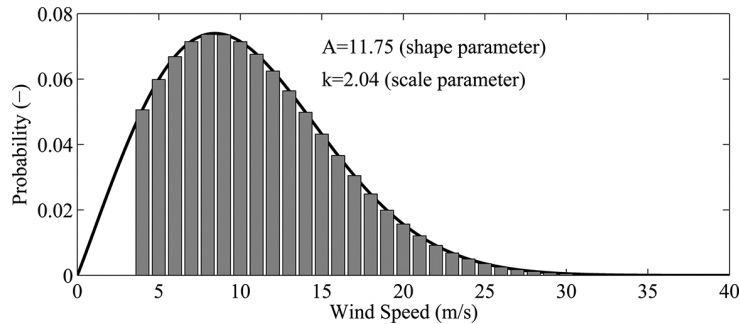


A=11.75 (shape parameter)
k=2.04 (scale parameter)

Figure 6: Weibull Velocity - probability Distribution

time in a year, that is

$$aep = N_{hours} \int_{V_{in}}^{V_{out}} f(u) P(u) du \tag{12}$$
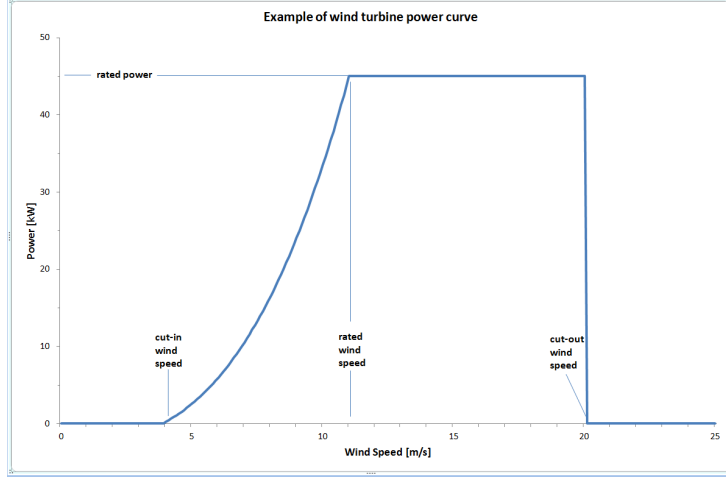
As it is known two main zones divide the curve.

Figure 7: Example Power Curve

- ZONE I, between cut-in and rated wind-speed, where $P = \frac{1}{2}C_P^{max}\rho\pi R^2 V_{wind}^3$

- ZONE II, between rated and cut-out wind-speed, where $P = P_{nominal}$

In ZONE I the HAWT is not working at its nominal power, but, it works at its highest efficiency $C_P^{max}$. As the wind speed increases so does the angular velocity to keep the same tip speed ratio $\lambda = \Omega R/V_{wind}$ and thus a similar power coefficient $C_P^{max}$. In fact, $C_P^{max}(\lambda, \theta_0, \mathbf{q})$ is function of the tip speed ratio and the angle of attack distribution given by pitch angle and (in a smaller amount) by the elastic dofs describing the deformation.Note that if we suppose a rigid blade, only one $C_P^{max}$ exists for every velocity in ZONE I, at a couple $\theta_{0C_P^{max}}$ and $\lambda_{C_P^{max}}$ to find, differently, it should be recomputed for every speed, that is for every consequent deformation status to be rigorous if elasticity is taken into account. In brief we have:

$$
\begin{cases}
C_P = C_P^{max}(\lambda_{C_P^{max}}, \theta_{0C_P^{max}}, \mathbf{q}) \\
\mathbf{q} = \mathbf{q}(V_{wind}) \\
\Omega = \lambda_{C_P^{max}} V_{wind}/R
\end{cases}
\tag{13}
$$

In ZONE II instead the nominal power has been reached and must be kept the same for different wind speed, also the angular velocity must be $\Omega_{nominal}$. So, to keep the same power and angular velocity, the blade pitch $\theta_0$ must be regulated in order to fulfill the following relations:

$$
\begin{cases}
C_P(V_{wind}) = P_{nominal}/(\frac{1}{2}\rho\pi R^2 V_{wind}^3) \\
\lambda(V_{wind}) = \Omega_{nominal} R/V_{wind}
\end{cases}
\tag{14}
$$

The regulation can follow two main roads:

- *Pitch Regulation* : that is profiles noses go towards the relative wind speed, so as to brake decreasing lift
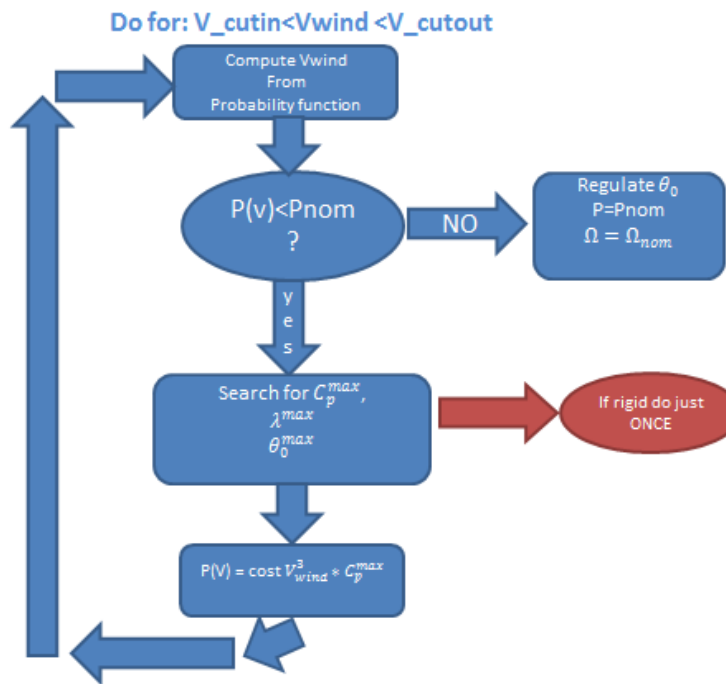
9
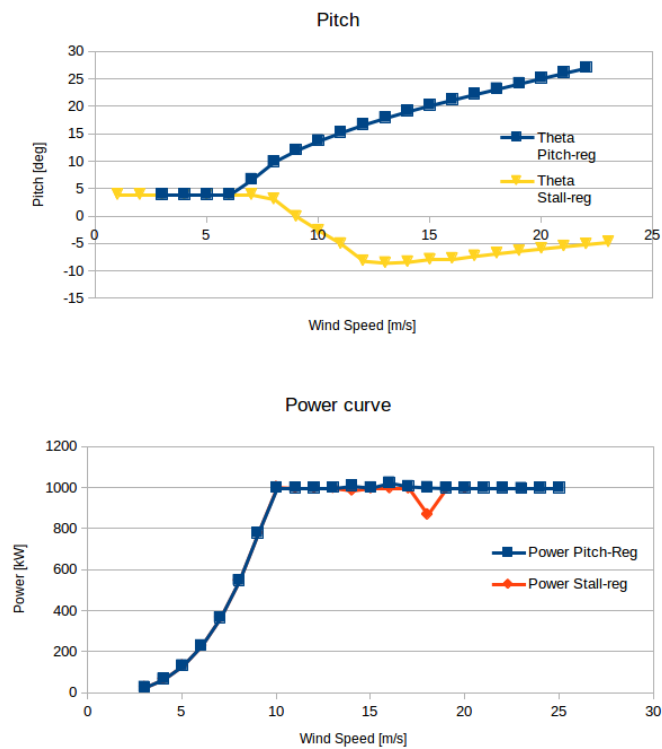
Figure 8: AEP logical Flowchart



Figure 9: Example of Pitch and Stall regulation by AEP module

- *Stall Regulation* :that is profiles noses get far from the relative wind speed, so as to brake by drag increase

### *Performance Optimization: Background*

Preliminary-design is indeed a critical stage, in which conceptual mistakes can compromise a lot of the final success. Concerning the design af HAWT, an iterative process is usually needed to merge a performing aerodynamic layout, namely twist, chord and thickness-ratio distributions, with the technical feasibility of the blade itself, and with the structural characteristics (e.g., stiffness and mass distributions) needed to pass all the requirements for certifications, usually verified by licensed complex codes. The iterative process can be very long and time-consuming, thus only the skill and the expertise of the designer can really speed it up. The amount of time that can be necessary for preliminary design can also be a limit as for the search of innovative configurations, since the easiest and shortest way often results to be following previous experience and adapting reliable layouts to new blades to design, with a few room for innovation. In the attempt to satisfy the need for speed and to simplify the overall design process, the assessment of the aeroelastic tool for performance optimization of HAWT (*POWT* from now on) required the introduction and application of an optimal design procedure for the definition of HAWT blades which generated maximum power. Since it is an inherently multidisciplinary, multi-dimensional constrained maximization problem, it is very challenging and characterized by non-linear multi-modal objective functions (i.e. functions with several local maxima in the design domain). Because of this, Genetic Algorithms (GAs) seem to be one of the more appropriate approaches to solve this optimization problem. Indeed, they are able to escape local maxima and to search for a global optimum, even in very complex issues, moreover they allow the implementation of very efficient/fast computational tools, as they are intrinsically suitable for parallel programming.

### Performance Optimization: The Genetic Algorithm

As already mentioned, in this work the blade optimization procedure is based on the application of a binary-based genetic algorithm developed by the authors [12, 13]. Genetic algorithms are probabilistic programming techniques that mimic the natural evolution in finding the optimal solution of a given problem [14]. In this process, potential solutions are called individuals and the whole set of individuals is called population. Each individual is identified by a string (chromosome) of binary digits (genes) ordered in a given sequence. The optimization procedure starts from a completely random-generated population and, at each step of the evolution process, individuals are quantitatively evaluated in terms of the corresponding value of the objective function. The population size in genetic algorithms is a crucial issue to consider when dealing with specific optimization problems, as it can seriously affect their efficiency. Indeed, a very small population (composed of few individuals) may lead to an unsatisfactory coverage of the problem domain, as well as to sampling errors [15], while a large population can lead to high computational time,

due to the number of evaluations of the objective function larger than necessary. Here, following Ref. [16], an estimate of the population size based on the variance of the objective functions is used.

Constraints are included in the optimization process through a quadratic extended interior penalty-function approach [17], which enhances the breeding possibility of individuals potentially able to generate good offspring. In this sense, constraints are taken into account indirectly, turning the constrained optimization process into a sequence of unconstrained minimization procedures. To build a new generation, the best individuals are selected on the basis of a fitness measure evaluated from the objective function and constraints. For the present analysis a tournament selection operator is used. It is based on a random selection of four parents, which are compared one-vs-one in two pairs and the couple of 'winners' are selected to be parents of two children with two independent crossover operations. A single random-point crossover operator is used.

Once the mate is performed, a binary uniform mutation operation is applied, to avoid premature convergence to local optima. This operator alters one or more binary digit (gene) in the chromosome by flipping it with a given probability. The amount of chromosome variations during the evolutionary process is controlled through a user-defined mutation probability factor, which is decreased during the optimization to reduce the impact of random mutations as the solution converges to an optimum. In order to prevent possible negative aspects of the evolution process and hence driving the solutions to get better over time, at each step of the optimization process the best individuals (a given, user-defined, percentage of the population size) are selected to become part of an elite group which is unchanged in the next generation. This technique, in addition to avoiding the possibility to obtain worse generation during the optimization process, enhances its convergence properties [18, 19]. The optimization procedure is iterated until either the chromosomes similarity (bit-string affinity) achieves a user-defined value [20], or the maximum number of iterations is reached.

**Performance Optimization: Structural Properties and Project Variables Definition**

Blade's structural characteristics were previously inserted into the *POWT* by means of an *ad hoc* database containing all the bidimensional properties of the section hosting the known aerodynamic profiles, which compose the blade. For each kind of profile the external shape were defined, while the structural features were given in a discrete manner in function of two parameters bound to the internal composition of the profile, with reference to Fig. 10 they were the overall skin-thickness $\epsilon$ and spar width L.

During this project the relation between section shape and the structural properties (e.g. stiffness, mass) for the aeroelastic analyses have been made far more realistic, integrating a module which links the real wing-box with the beam sections in the aeroelastic simulations. According to the present criteria the starting (fixed) point to define the blade is the definition of the section in terms of:
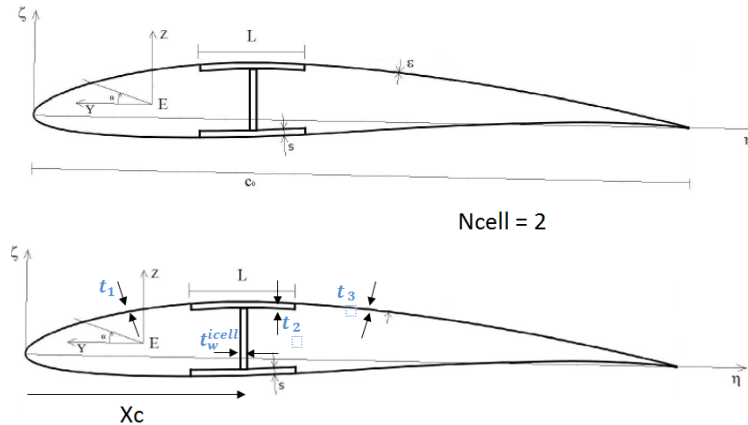
12

Figure 10: Blade box structural sketch

- materials and plies disposition and orientation

- the number $N_P$ and kind of profiles to spread in a right sequence depending on their thickness ratio

Once this is decided the new set of overall project variables is composed by the sum of $N_P$-sections and some blade-global properties.
The blade global properties are:

- The number of cells Ncell;

- The constant spar-width L (note that spar is allowed to reach up to 80% of blade length and that compliance with the chord dimension is always ensured)

The section properties, defined for $N_P$ profiles are:

- $t_1$, the skin thickness in the upper and lower nose part;

- $t_2$, the skin and spar-width thickness in the upper and lower central part, it is the main definer of structural stiffness;

- $t_3$, the skin thickness in the upper and lower tail part;

- $t_w^{icell}$, the vertical webs' thickness, of course they are always $N_{cell} - 1$;

- $X_c$, is the distance between the middle of the spar-width and the leading edge (a check is always made in the code to ensure that geometry is consistent with reality, i.e. the spar is contained into the cell);

- c, the section chord;

- $\theta_x$, the section twist angle (this variable is not accounted for in circular sections)

- $y_p$, the profile position (of course these are $N_P - 1$ because the first and the last positions are locked);

The needed section's properties are:

- Section mass $m[\frac{kg}{m}]$

- Axial stiffness $EA[N]$

- Shear center position w.r.t. Leading edge position $(Y_e, Z_e)[m]$

- Aerodynamic center position w.r.t. Leading edge position $(Y_a, Z_a)[m]$

- Centroid position w.r.t. elastic center $(\eta_c, \zeta_c)[m]$

- C.G. w.r.t. elastic center $(\eta_c, \zeta_c)[m]$

- Radius of giration w.r.t. principal axes $R_1$ and $R_2$ $[m]$, together with principal axis angular position $\alpha_R[deg]$ w.r.t. chord.

- Bending stiffness $EI_\eta$ and $EI_\zeta$ $[Nm^2]$, together with figure axis angular position $\alpha_{EI}[deg]$ w.r.t. chord.

- Torsional stiffness $GJ$ $[Nm^2]$

The plies disposition was analysed using the structural modul of the commercial code FOCUS6. It is a FEM tool for the structural analysis of HAWT blades, which also provides as output the section properties. The analysed profiles were DELFT40, DELFT30, DELFT35, DELFT25, DELFT21 and NACA64-618. Further, two typical kind of root section were used:

- a circular section, characterized by higher skin thickness

- a transitional, quasi-circular section between the circular one at the root, and the section with maximum chord. Here, a profile was chosen with maximum thickness equal to 85 % of the chord, whose geometry is an average value between circular section and the DELFT40 profile.

**Performance Optimization: The Optimal Blade-design Procedure**

As stated in the agreement with AW, the optimization process is here applied to design a HAWT-blade with different users options.

1. $C_P$ optimization means that a fixed operative condition in terms of $\theta_0$ (usually $= 0$) and $\lambda$ is chosen. This choice is usually based on the experience of the designer to be as closer as possible to a desired possible maximum among the different $C_P(\lambda, \theta_0)$ curves, whose historical database is differentiated in terms of wind turbine's model, as seen in Fig 12

2. $aep$ optimization, of course far more time-consuming, use as objective function the annual energy. This choice ensures the power curve to be assessed with actual $C_P^{max}$ and maximum turbine efficiency. In turn, in this case the user can choice:
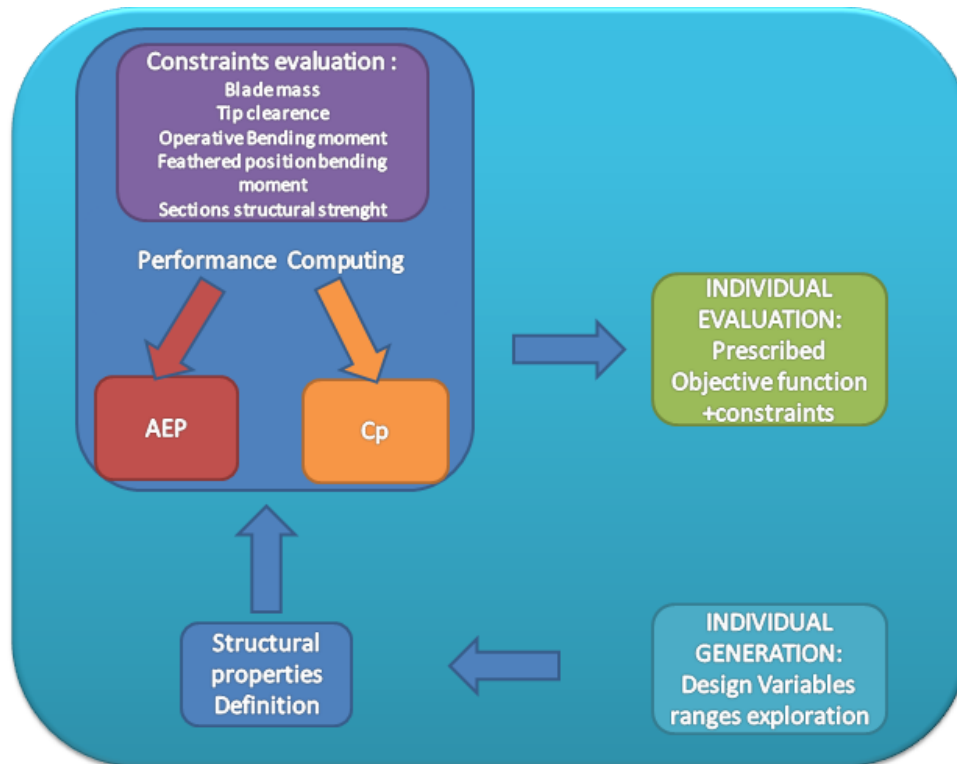
Figure 11: Optimization Design Process Schematics

- High-speed solution: A chosen $C_P$ (if the maximum is known) is used to draw the power curve, here the design by $aep$ does not change anything with respect to $C_P$ but the visualized output

- Medium-Speed solution : The real $C_P^{max}$ is computed, with the assumption of rigid blade, which means to search for it just once in the ZONE I described in the above sections.

- Slow-speed: $C_P^{max}$ is computed for every wind speed in ZONE I, accounting for elasticity.

Note that the AEP module, when set to 'Design' does not waste time in the search of the $\theta_0$ pitch values to keep nominal power.

Besides the described design variables, new constraints have been defined and added. It is worth to remark that in this kind of procedures constraints, as well as the objective function are very easy to change, as they actually are some *numbers* with which the aeroelastic tool and the optimizer code exchange information between them. Up to now the code can consider:

- Blade-weight

- Tip-clearance when passing by the pylon

- Blade bending moment in operative condition
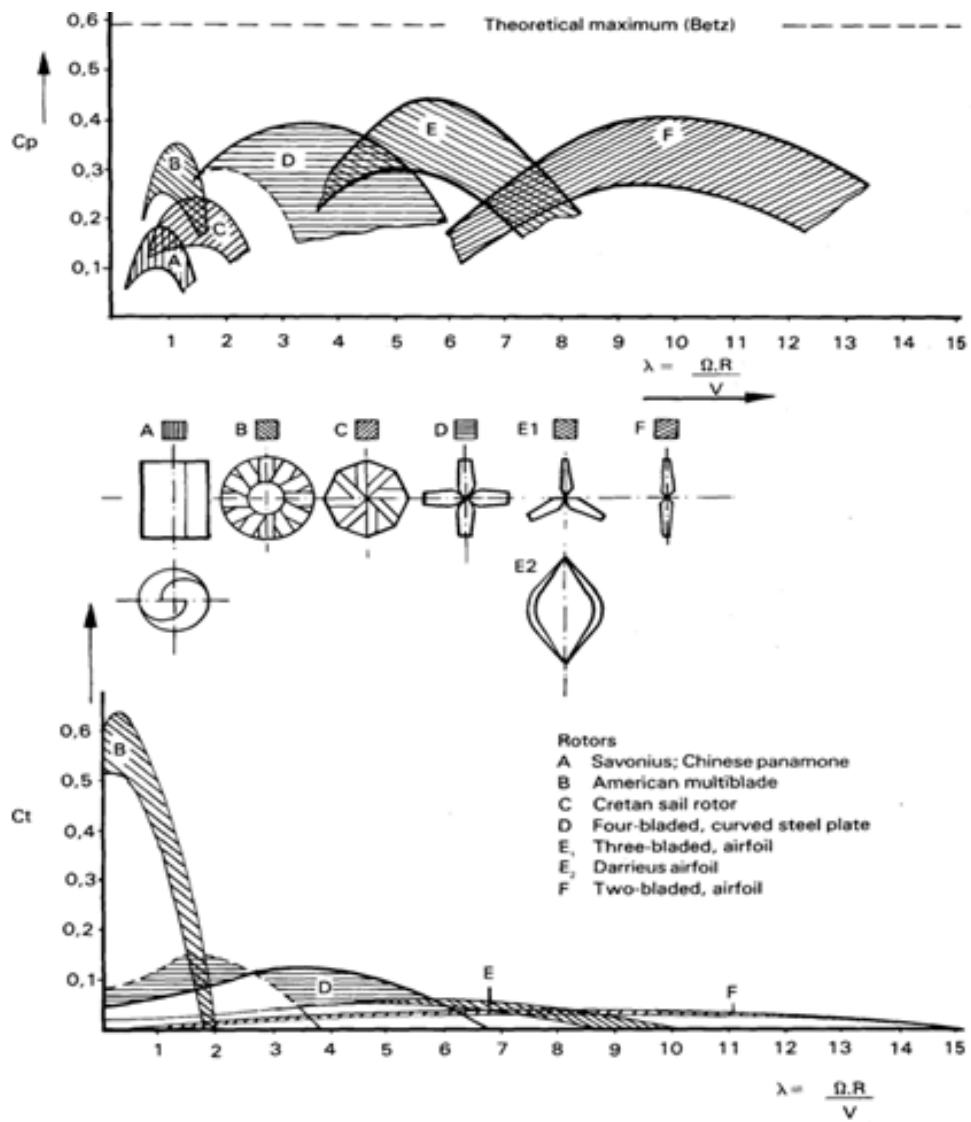
- Blade bending moment in feathered position

15

Figure 12: Trends of Wind Turbine Cp curves

- section strength analysis by standard failure criteria

Following the genetic algorithm described above, design variables are explored starting from random values taken between imposed boundaries (the setting of these boundaries is indeed an important issue as it determines the range of solutions examined).
Finally it must be highlighted that for the sake of accuracy it was decided to interpolate the profiles shapes (not the structural properties directly) along the whole span, and only then to compute the structural properties, function of the interpolated geometry.

### GUI Development

Part of the development effort of this project was spent in the creation of a unified graphical user interface (GUI) giving access to all the main functions of Tiltaero. The aim of the GUI is to lower the entry barrier for new users while allowing existing users to use TA more effectively. The GUI was developed using the Python 2 programming language and the Qt 4 toolkit, in particular using the PyQt wrappers. The Python programming language was chosen to allow a fast and agile development of both the GUI and of all the code needed to interact with the TA. Its license permits its use for commercial products, however if an effective obfuscation of the GUI code is desired, the conversion of the GUI code to C++ is advised. The Qt toolkit library represent the de facto standard for the development of multi platform GUIs. The use of the Qt library in a closed source commercial product is permitted by two different licenses alternatively. The first option is to use the LGPL 2.1 license with its limitations, whereas a second option would be acquiring a commercial license from Digia. The PyQt wrapper library is the only part of the software stack that needs a commercial license to distribute a closed version of the GUI. However the alternative PySide was not deemed sufficiently mature and stable for this project. For the graphical visualization of two dimensional data the Matplotlib library was used. This choice was driven by the high quality of the visualization and by the good integration it provides with the rest of the libraries used in this project. As underlying format for GUI save files the HDF5 format specification was used. At this stage development only the input data is saved on the files, whose extension was chosen as *.wwf*; however the the HDF5 format was chosen to allow an efficient storage of output results. A schematic summary of all the current software dependencies is presented in table 2. Although the GUI was developed and tested on a Linux platform, all these library are multiplatform and compatible with Windows and OS X operating systems, and its code was written to be portable across all the mentioned operating systems. The GUI is based on a project-centric paradigm. The user, when starting a new project can chose between creating a new analysis project or a new optimization project. When a new analysis project is created the user has the option to define a new turbine design or to use an existing one. In the former case a new tab is opened with a default turbine design and the user

17

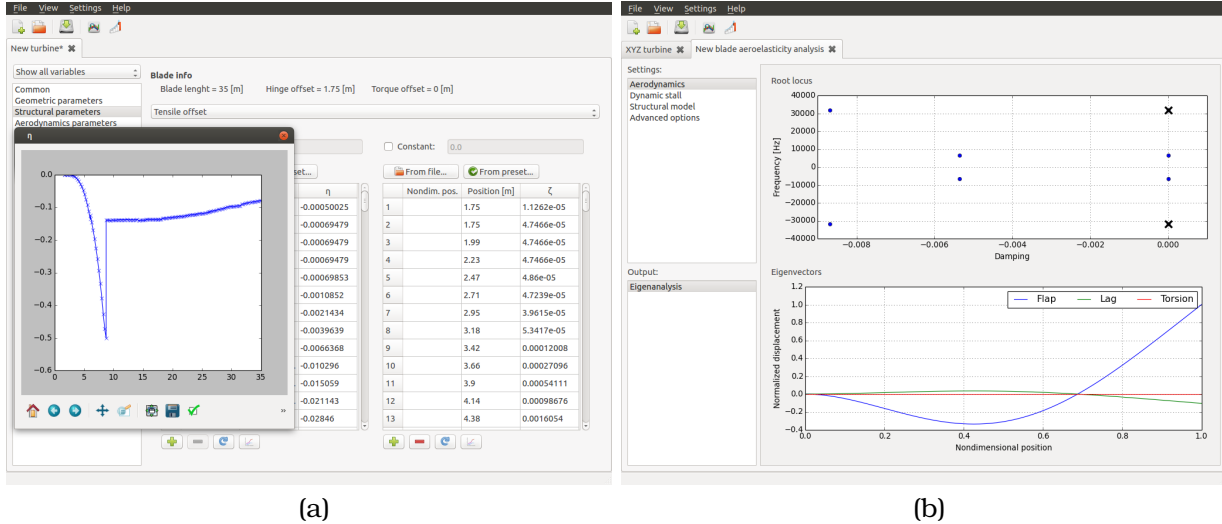| Name | Usage | Web site |
|---|---|---|
| python 2.7 | Programming language | python.orgpython.org |
| Qt 4.8 | GUI toolkit | qt-project.orgqt-project.org |
| PyQt 4.10 | Python Qt wrapper | riverbankcomputing.com/software/pyqt |
| matplotlib 1.2 | Plotting library | matplotlib.orgmatplotlib.org |
| h5py | Python HDF5 wrapper | h5py.orgh5py.org |

Table 2: Software dependencies



(a)  (b)

Figure 13: Two screenshots of the GUI showing (a) the input interface and (b) the output interface for an aeroelastic eigenvalues analysis

can modify all the parameters defining the geometric, structural and aerodynamic characteristics of the turbine (see Fig. 13a). After a new turbine is defined, or an existing design is opened, the user can chose the analysis to perform among six different analysis types. Each analysis has its own set of configuration parameters. These parameters are organized in categories and a default setting is provided. The work-flow is designed to let the user obtain a result as efficiently as possible. When a new analysis project is created the default settings are inherited from the previous analysis. In this way it is very easy to perform and compare two similar analysis modifying just few parameters. Moreover using this approach it is possible to perform the same analysis on several turbine design without the need of redefining all the analysis parameters. For the optimization project a similar approach is employed. The user can modify to all the optimizer parameters in a special tab and the optimization results are presented in a special section of the same tab. After an optimized configuration is found it can be exported in a design file and analyzed in an analysis project. For both the optimization and the analysis projects the GUI takes care of setting all the necessary configuration files of TA and of retrieving the correct output files.

# References

[1] *"Assessment of an Aeroelastic Solver for the Optimization of HAWT"* ,University Roma Tre, Technical Report, January 2012.

[2] *"Assessment of an Aeroelastic Solver for the Optimization of HAWT, Final Report"* ,University Roma Tre, Technical Report, January 2013.

[3] Hodges D.H., Dowell E., *"Nonlinear equation of motion for the elastic bending and torsion of twisted non uniform rotor blades"*, December 1974 , NASA Technical Report D7818

[4] Hodges, D.H., Ormiston, R.A., *"Stability of Elastic Bending and Torsion of Uniform Cantilever Rotor Blades in Hover with Variable Structural Coupling"*, NASA TN D-8192, April 1976.

[5] Hodges D.H., Dowell E., *"Nonlinear equation of motion for the elastic bending and torsion of twisted non uniform rotor blades"*, December 1974 , NASA Technical Report D7818

[6] Molica Colella M. (2010), *"Risposta e Stabilita' di Velivoli Tiltrotor"*, *PhD Thesis (in italian)* , University Roma Tre, Rome, Italy

[7] Leishman, J.G., and Beddoes, T.S., *âA Semi-Empirical Model for Dynamic Stallâ*, J. Am. Helicopter Soc., Vol. 34, no. 3, 1989, pp. 3 â 17

[8] Calabretta, A., Molica Colella, M., Greco, L., Dubbioso, G., Testa. C. and Gennaretti, M., *'A comprehensive numerical model for horizontal axis wind turbines aeroelasticity'*, Proceedings of the Conference on Wind Energy Science and Technology, 2013, Ankara (Turkey).

[9] Calabretta, A., Molica Colella, M., Greco, L. and Gennaretti, M., *'Assessment of aerodynamics models for wind turbines aeroelasticity'*, Proceedings of the 2014 World Congress on Advances in Civil, Environmental, and Materials Research (ACEM14), 2014, Busan (South Korea).

[10] C. Lindenburg *'Investigation into Rotor Blade Aerodynamics - Analysis of the stationary measurments on the UAE phase-VI rotor in the NASA-Ames wind tunnel'*, ECN-C–03-025, July 2003

[11] J.C. Dai, Y.P. Hu, D.S. Liu, X. Long, *"Aerodynamic loads calculation and analysis for large scale wind turbine based on combining BEM modified theory with dynamic stall model"'*, Renewable Energy, Elsevier

[12] G. Bernardini, C. Testa, M. Gennaretti, *"Optimal Design of Tonal Noise Control Inside Smart-Stiffened Cylindrical Shells"*, Journal of Vibration and Control, Vol. 18, No. 8, SAGE (2012), pp. 1233-1246.

[13] D. Calcagni, G. Bernardini, F. Salvatore, *"Automated Marine Propeller Optimal Design Combining Hydrodynamics Models and Neural Networks"*, Proceedings of 11th International Conference on Computer Applications and

Information Technology in the Maritime Industries, Liege, Belgium, 2012 April 16-18, Venice (2011).

[14] J.H. Holland, *"Adaptation in Nature and Artificial Systems"*, University of Michigan Press, Ann Arbor (1975).

[15] R.E. Smith, E. Smuda, *"Adaptively Resizing Populations: Algorithm, Analysis, and First Results"*, Complex Systems, Vol. 9, No. 1, Complex Systems Publications, Inc. (1995), pp. 47-72.

[16] D.E. Goldberg, *Optimal Initial Population Size for Binary-Coded Genetic Algorithms*, (TCGA Report No. 85001). University of Alabama, Tuscaloosa, Ala. : Clearinghouse for Genetic Algorithms, Dept. of Engineering Mechanics, Tuscaloosa (1985).

[17] R.T. Hatfka, Z. Gurdal, *"Element of Structural Optimization"*, Kluwer Academic Publishers, Dordrecht (1992).

[18] G. Rudolph, *"Evolutionary Search Under Partially Ordered Sets"*, (Tech. Rep. CI-67/99) Univ. Dortmund, Dept. Comput. Sci./LS11, Dortmund (1999).

[19] E. Zitzler, K. Deb, L. Thiele, *"Comparison of Multiobjective Evolutionary Algorithms: Empirical Results"*, Evol. Comput., Vol. 8, No. 2, PubMed (2000), pp. 173-195.

[20] D.P. Raymer, *"Enhancing Aircraft Conceptual Design Using Multidisciplinary Optimization"*, PhD Thesis, Royal Institute of Technology, Stockholm (2002).